SIMULATION OF THE MICROBUNCHING INSTABILITY IN BEAM DELIVERY SYSTEMS FOR FREE ELECTRON LASERS

I. Pogorelov[#], NICADD, DeKalb, IL 60115, U.S.A.

J. Qiang, R. Ryne, M. Venturini, A. Zholents, LBNL, Berkeley, CA 94720, U.S.A.

R. Warnock, SLAC, Stanford, CA 94025, U.S.A.

Abstract

In this paper, we examine the growth of the microbunching instability in the electron beam delivery system of a free electron laser (FEL). We present the results of two sets of simulations, one conducted using a direct Vlasov solver, the other using a particle-in-cell code Impact-Z with the number of simulation macroparticles ranging up to 100 million. Discussion is focused on the details of longitudinal dynamics and on numerical values of uncorrelated (slice) energy spread at different points in the lattice. In particular, we assess the efficacy of laser heater in suppression of the instability, and look at the interplay between physical and numerical noise in particle-based simulations.

PHYSICAL SETTING

The FEL beam delivery system layout used in our study was that proposed for the FERMI@Elettra accelerator [1]. As shown in Fig. 1, it consisted of an injector, four linacs (for a total of 15 RF cavities), a laser heater, two bunch compressors, and a spreader used to direct the beam into one of two undulator lines. (The starting point for all the
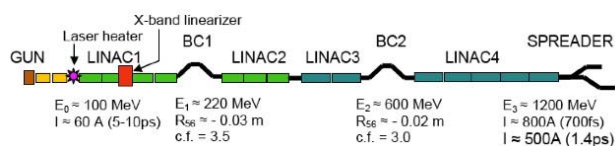

Figure 1: Beam delivery system lattice proposed for the FERMI@Elettra FEL and used in our simulations.

simulations presented here was the laser heater rather than the injector gun.) We considered two electron bunch configurations: the "medium bunch" of charge 0.8 nC and initial length ~0.7 ps; and the "long bunch" of charge 1.0 nC and initial length ~1.4 ps. In both cases, the electron bunch had a peak current ~70A and energy of about 100 MeV at the laser heater, and was accelerated to approximately 1.2 GeV by the time it reached the spreader. A net factor of 10 compression was realized in both cases. Preservation of the beam quality during bunch compression and acceleration requires suppression of the longitudinal space charge-(LSC-) and coherent synchrotron radiation-(CSR-)driven microbunching instability. To this end, a laser heater was proposed [2] that would increase the uncorrelated rms energy spread in the bunch and thus "wash out", through a mechanism analogous to Landau damping, what microstructure may initially be present in the distribution. (In our simulations, a slice energy spread is introduced to mimic the presence

[#]ilya@nicadd.niu.edu

of the laser heater; a more accurate model is currently under development).

CODES USED IN THE SIMULATIONS. MODELING COLLECTIVE EFFECTS

Numerical simulations presented here were conducted using two codes that model Vlasov-Poisson systems: the particle-in-cell code Impact-Z, and a recently developed direct Vlasov solver. Impact-Z is a parallel, fully 3D beam dynamics code whose features relevant to modeling high brightness electron beams include a 3D, self-consistent space charge model, 1D CSR model, RF structure wake fields, effects related to nonlinear magnetic optics, and the integrated Green's function algorithm for solving the Poison equation in high aspect ratio beams. A detailed description of the code can be found in [3]. The direct Vlasov solver uses (nonlinear) Vlasov equation to follow the evolution of the 2D distribution function in the longitudinal phase space of the beam. 4D effects are accounted for by including a factor in the distribution function that depends on transverse action. The code's key advantages include high speed and the absence of sampling noise (as distinct from discretization/gridding noise). A complete description of the code is given in [4].
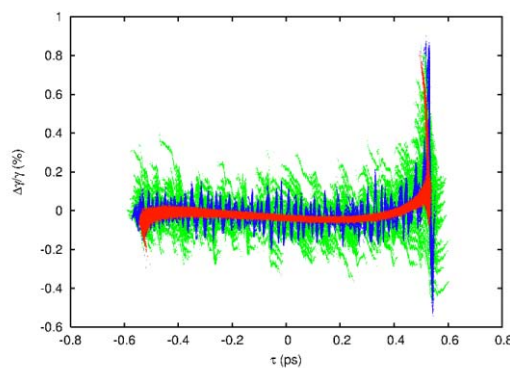

Figure 2: Microbunching instability seen in the longitudinal phase space of the bunch at the end of LINAC4 in Impact-Z simulations with 2M particles (green) and 100M particles (blue) with CSR turned off, compared with the no-space-charge, no-CSR result (red).

Two central challenges in modelling the microbunching instability are 1) validating the space charge and CSR models, and 2) distinguishing the effects due solely to sampling noise (in particle-based simulations) from those due to the physical microstructure in the actual bunch that

consists of a much larger, but finite, number of electrons. As illustrated in Fig. 2, over- or underestimating either the sampling noise or collective effects in computational modelling of the instability can have a dramatic effect on the overall simulation fidelity.

Turning to the models' specifics, in the direct Vlasov solver a 1D space charge wake is used that assumes the impedance model derived for a bunch with transversally uniform density and circular cross-section:

$$\hat{Z}(k) = \frac{iZ_0}{\pi \gamma r_b} \frac{1 - xK_1(x)}{x} \Big|_{x=kr_b/\gamma},$$

where $K_1(x)$ is a modified Bessel function and $Z_0 = 120\pi$ Ω, the vacuum impedance. The code uses a 1D, free-space, steady-state CSR wake model with impedance per unit length

$$\hat{Z}(k) = Z_0 \frac{\Gamma(2/3)}{3^{1/3}4\pi R}(\sqrt{3} + i)(kR)^{1/3}.$$

The details are given in [4].

A CSR model recently implemented in IMPACT is based on the 1D (zero transverse emittance), steady-state (long magnet, no transient effects) result of Ref. [5], where the change in energy due to CSR is given by

$$\frac{dE}{cdt} = -\frac{2e^2}{3^{1/3} R^{2/3}} \int_{-\infty}^{s} \frac{ds'}{(s-s')^{1/3}} \frac{d\lambda(s')}{ds'}.$$

Numerical evaluation of this expression is complicated by the fact that the integral operator kernel is weakly singular, and the linear charge density $\lambda(s)$ is contaminated by numerical noise. The magnitude of this noise depends both on the number of simulation particles and number of grid points and, in practice, substantially exceeds the level of noise found in the physical system being modeled; filtering provided by the charge deposition process alone is not sufficient.
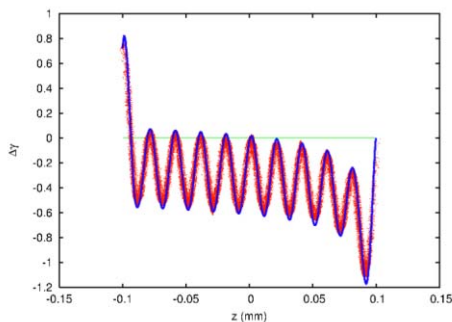

Figure 3: Testing the CSR routine on a single-magnet, sinusoidally-modulated flat-top initial density distribution model. Numerical result with 2M test particles (red), analytical prediction (blue), and the initial distribution (green) are shown in the longitudinal phase space.

Our approach is based on 1) a combination of integration-by-parts, 2) use of computationally efficient custom-designed filters that conserve charge, preserve the positivity of the distribution function, and are characterised by transfer functions that uniformly approach zero as $\omega \rightarrow \omega_{Nyquist}$, and 3) treating differently--for the purposes of numerical integration--the regions near and far from the singularity of the integral term's kernel. The algorithm is described in more detail in [6]; Fig. 3 shows the results of one of several validation tests.

PARAMETRIC STUDIES OF THE MICROBUNCHING INSTABILITY

Our parametric studies of the instability involved varying the value of σ_{E0} the rms slice energy spread produced by the laser heater, and--in particle simulations--the number of macroparticles.
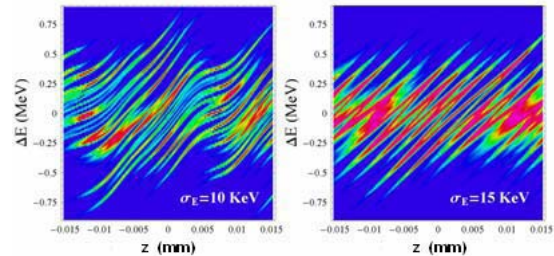

Figure 4: Longitudinal phase space in simulations with the direct Vlasov Solver for two choices of the initial rms slice energy spread.

To study the efficacy of the laser heater in mitigating the instability, we conducted IMPACT simulations with σ_{E0} = 7.7, 15.3, and 22.1 keV (with the number of simulation particles ranging from N = 2M to 100M), and Vlasov simulations with σ_{E0} = 7.5 and 15.3 keV (where the magnitude of the noise artificially added to the initial distribution was chosen so as to match shot noise in the actual bunch composed of 4.5B electrons). A 64x64x2048 Cartesian grid was used for all IMPACT simulations discussed in this paper so as to resolve with certainty the range of spatial frequencies where most of the gain occurs. As expected, weaker/slower instability growth is seen at higher σ_{E0}. In addition, we found that even with the laser heater present, the instability growth is sufficiently strong for the nonlinear saturation to be reached relatively early in the beamline; this means that particle-based simulations and/or solvers based on fully nonlinear models are required to accurately model the dynamics in longitudinal phase space in this regime where linear theory is no longer applicable. Fig. 4 illustrates some of these points.

Increasing the number of simulation particles results in the reducing the sampling noise in the charge distribution function and leads to improved modelling of the instability. Initial distributions were produced from a 200k-particle "template" distribution obtained in separate injector-to-laser heater simulations with the code Astra [1]. This distribution, with the energy-z correlation subtracted, is shown in Figs. 5 and 6; note the significant amount of irregular microstructure due largely to a low particle count. So as to focus on effects due to the

sampling noise, a smooth approximation to the uncorrelated part of the longitudinal phase space distribution was constructed as the direct product of the denoised bunch current and a smoothed projected "energy profile"; it was then sampled by rejection method with up to 100M particles. Transverse distribution was produced by replicating the "template" transverse distribution.
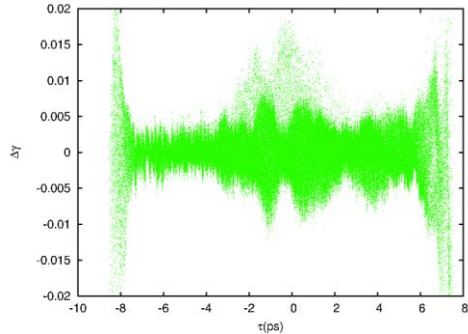

Figure 5: The uncorrelated part of the longitudinal phase space distribution at the entrance to the laser heater, before a smooth approximation is constructed.
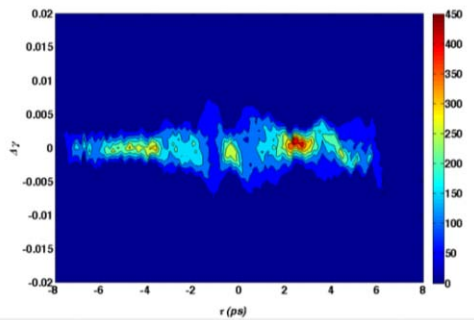

Figure 6: Same as Fig.5 except showing local particle number density.

The results of IMPACT simulations with N = 2, 6, 20, 60, and 100M macroparticles and two different values of σ_{E0} are summarized in Table 1 and illustrated in Fig. 7 and 8.

Table 1: Final Slice rms Energy Spread σ_E

N	$\sigma_{E0} =$7.7 keV	$\sigma_{E0} = $15.3 keV
2M	$\sigma_E = 940$ keV	$\sigma_E = 710$ keV
6M		690 keV
20M	530 keV	540 keV
60M		420 keV
100M	360 keV	320 keV

A careful analysis of the results shows that extrapolation to the actual number of electrons (4.5B) is tentative at best. Work in progress that will be reported elsewhere includes enabling larger-scale simulations and new approaches to separating the contribution to σ_E that is due solely to sampling noise.
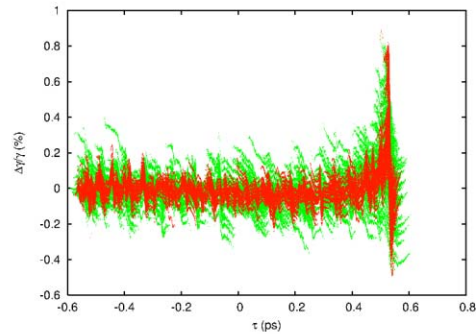

Figure 7: Results of IMPACT simulations with σ_{E0}=7.7keV and varying number of particles sampling the same initial distribution: 2M (green) vs. 20M particles (red). The final distribution's footprint in the longitudinal phase space of the bunch is shown.
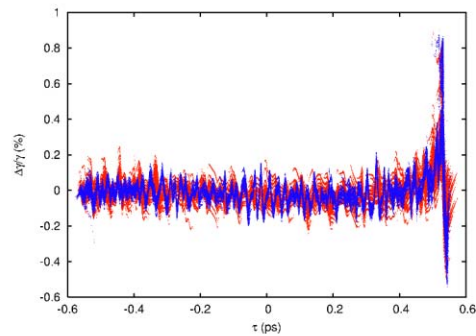

Figure 8: Same as Fig. 7 for 20M particles (red) and 100M particles (blue).

A thorough discussion of this and other related work will be given in an upcoming publication.

REFERENCES

[1] M. Cornacchia et al, Paper LBNL-60958, http://repositories.cdlib.org/lbnl/LBNL-60958
[2] Z. Huang *et al.*, *Phys. Rev. ST Accel. Beams* **7**, 074401 (2004).
[3] J. Qiang, R. Ryne, S. Habib, and V. Decyk, *J. Comp. Phys*. **163**, 434 (2000).
[4] M. Venturini, R. Warnock, and A. Zholents, *Phys. Rev. ST Accel. Beams* **10**, 054403 (2007).
[5] E.L. Saldin, E.A. Schneidmiller, and M.V. Yurkov, *Nucl. Instrum. Methods Phys. Res.*, *Sect. A* **398**, 373 (1997).
[6] I. Pogorelov *et al.*, in *Proc. 9th Int. Comput. Accel. Phys. Conf.*, WEPPP01, 182 (2006).